Solution-Processible Carbazole Dendrimers as Host Materials for Highly Efficient Phosphorescent Organic Light-Emitting Diodes

Jiuyan Li, Ting Zhang, Yunjing Liang, and Ruixia Yang*

A group of dendrimers with oligo-carbazole dendrons appended at 4,4′-positions of biphenyl core are synthesized for use as host materials for solution-processible phosphorescent organic light-emitting diodes (PHOLEDs). In comparison with the traditional small molecular host 4,4′-N,N′-dicarbazolebiphenyl (CBP), the dendritic conformation affords these materials extra merits including amorphous nature with extremely high glass transition temperatures (ca. 376 °C) and solution-processibility, but inherent the identical triplet energies (2.60–2.62 eV). In comparison with the widely-used polymeric host polyvinylcarbazole (PVK), these dendrimers possess much higher HOMO levels (–5.61 to –5.42 eV) that facilitate efficient hole injection and are favorable for high power efficiency in OLEDs. The agreeable properties and the solution-processibility of these dendrimers makes it possible to fabricate highly efficient PHOLEDs by spin coating with the dendimers as phosphorescent hosts. The green PHOLED containing $Ir(ppy)_3$ (Hppy = 2-phenyl-pyridine) dopant exhibits high peak efficiencies of 38.71 cd A^{-1} and 15.69 lm W^{-1}, which far exceed those of the control device with the PVK host (27.70 cd A^{-1} and 9.6 lm W^{-1}) and are among the best results for solution-processed green PHOLEDs ever reported. The versatility of these dendrimer hosts can be spread to orange PHOLEDs and high efficiencies of 32.22 cd A^{-1} and 20.23 lm W^{-1} are obtained, among the best ever reported for solution-processed orange PHOLEDs.

1. Introduction

Phosphorescent organic light emitting diodes (PHOLEDs) containing transition metal complexes as emitters have attracted much research and industry attention since they are capable to utilizing excitons in both singlet and triplet states and may achieve nearly 100% internal quantum efficiency.[1–3] In order to suppress the severe concentration quenching and triplet-triplet annihilation that otherwise exist in neat films, the metal complex phosphors are typically doped in a certain host material or mixture in PHOLED.[4,5] Therefore, the host plays an essential role in determining the device performance and even the production cost. In principle, an ideal phosphorescent host material should possess the following attributes: (1) a certain charge transporting ability to facilitate electrical conduction of the whole device; (2) appropriate highest occupied molecular orbital (HOMO) and lowest unoccupied molecular orbital (LUMO) levels to guarantee efficient charge injection into this emitting layer from the adjacent layers and, thus, as low driving voltages as possible; (3) a suitably high triplet energy to guarantee efficient forward energy transfer from the host to the metal complex dopant and to prevent reverse energy transfer. Furthermore, the small molecular or polymeric nature of the host material is the primary factor that determines the fabrication method of the emitting layer and the entire OLED. Until now, many PHOLEDs have been fabricated by vacuum thermal co-evaporation with phosphor emitter doped in a certain small molecular host,[6,7] which requires complicated technological processes and the unavoidable waste of a large amount of organic materials, leading to relatively high fabrication costs. It is generally believed that solution-based processes, such as spin-coating or ink-jet printing, will be required for the fabrication of low-cost, large-area OLED display or lighting products.[8,9] To date, solution-processed PHOLEDs have mainly been produced from polymeric materials by incorporation of iridium complexes either by physical blending in polymeric host materials, such as polyvinylcarbazole (PVK)[10–12] and polyfluorene (PFO),[13] or chemical bonding on polymer chains.[14,15] A large number of PHOLEDs with PVK as a triplet host for iridium complex phosphors have been reported, many of them achieving good electrophosphorescence performance.[10–12] However, the polymeric materials have their intrinsic disadvantages, such as uncertain molecular structure and difficulty in purification (the purity of materials has a great influence on their electroluminescence

Dr. J. Li, T. Zhang
State Key Laboratory of Fine Chemicals
School of Chemical Engineering
Dalian University of Technology
2 Linggong Road, Dalian 116024, China
E-mail: jiuyanli@dlut.edu.cn
Y. Liang, R. Yang
School of Chemistry
Dalian University of Technology
2 Linggong Road, Dalian 116024, China

DOI: 10.1002/adfm.201201326

performance). In particular, the most widely-used phosphorescent host PVK has a low HOMO level of –5.8 eV,[16] which has a large hole barrier with the ITO (work function = –4.8 eV) anode or the typical hole injecting layer poly(3,4-ethylenedioxythiophene): poly(styrenesulfonate) (PEDOT:PSS) (HOMO = –5.2 eV).[17] Consequently the PVK-based devices usually have relatively high turn-on voltages and driving voltages, which are not favorable for high power efficiencies of the devices.[18] Most recently, there have been several reports exploring small molecular materials as triplet hosts to fabricate PHOLEDs by spin coating.[19,20] Although acceptable performance was obtained, the device stability is still a concern because of the comparatively lower glass transition temperatures and inferior film forming ability of the solution techniques, especially when large area application is taken into account.

Dendrimers may be ideal altenatives to polymers, serving as triplet hosts in solution-processed PHOLEDs. Dendritic molecules possess many advantages[21,22] such as repeatable monodispersity and high levels of purity like small molecules, which are essential for ideal device performance. In addition, they possess high molecular weight and good solubility in common organic solvents like polymeric materials, which make them suitable for solution methods to prepare thin films and OLEDs. Furthermore, the dendritic molecules are usually amorphous with high glass transition temperatures (T_g) based on their large molecular weight and bulky steric conformation, which is really a valuable merit for host material if high device stability is desired. Therefore, dendritic molecules with good solubility and film morphology for solution-processible phosphorescent light-emitting devices, either as hosts or doped emitters, have been investigated.[23,24] The first report of dendritic molecules used as efficient solution-processible hosts for triplet emitters was published by Wang et al.[23] They adopted carbazole-based conjugated dendrimers as the host and blue-emitting iridium(III)bis(4,6-(difluorophenyl) pyridinato-N,C$^{2'}$)picolinate (FIrpic) as the guest to prepare the emitting layer by spin coating, achieving a maximum power efficiency of 15.4 lm W^{-1} (27.6 cd A^{-1}, 12.7%) for double layer devices. The efficiency of the blue electrophosphorescent device with the dendrimer host was 86% higher than the PVK-based device. Dendritic host materials for green PHOLEDs, however, have received little attention in the literature. Yang et al. reported solution-processed green PHOLEDs using a new carbazole dendrimer as the host in the emitting layer, which is the only example of using a dendrimer host for green PHOLEDs reported thus far.[24a] However, the maximum luminance efficiency was reported to be only 16.8 cd A^{-1}.

Inspired by the solution-processed PHOLED trend and the potential benefits of dendritic host materials, our interest is to explore novel dendrimer materials with excellent properties for application in solution-processed PHOLEDs. The dendrimers reported in present paper, **G1**, **G2**, and **G3** (**Scheme 1**), have the same molecular skeletons as 4,4′-N,N′-dicarbazolebiphenyl (CBP), in which the twisted biphenyl core and the bulky dendrons are expected to lead to a nonplanar three-dimensional molecular conformation.[25] It is well established that CBP is one of the most successful triplet host materials used in PHOLEDs.[26,27] However, the small molecular nature of CBP means that it is only possible to prepare PHOLEDs by vaccum techniques. In these dendritic CBP derivatives, the individual carbazole is selected as the dendron and the whole dendrimer grows up to higher generation in such a way that the outer carbazole is attached via its N-position directly on the 3- and 6-positions of each inner carbazole moiety. The experimental data revealed that such a dendron design strategy does not obviously influence the triplet energy of the resultant dendrimers.[28] In order to ensure good solubility and film-forming ability using wet methods for the desired dendrimers, their peripheral carbazoles were decorated by *tert*-butyl groups. Electroluminescence investigation revealed that, similar to CBP, these novel dendrimers serve as excellent triplet hosts for green and orange emitting iridium complexes in PHOLEDs. However, they are advantageous over CBP because they are suitable for solution-processing to make OLEDs. In comparison with the traditional solution-processible PVK host, all these dendrimers are superior in terms of their higher HOMO levels and easier hole injection. The green and orange-emitting PHOLEDs using **G2** as the host exhibited the maximum luminance efficiency (η_L) of 38.71 cd A^{-1} (corresponding to a maximum power efficiency of 15.69 lm W^{-1}) and 32.22 cd A^{-1} (20.23 lm W^{-1}), respectively, which far exceed those of the best devices with PVK hosts.

2. Results and Discussion

2.1. Synthesis

The synthetic routes for the carbazole-based dendritic molecules (**G1**, **G2**, **G3**) are shown in Scheme 1. The synthesis of G1 was previously reported.[29] First, the important intermediates including the first- to third-generation dendrons, **D1**, **D2**, and **D3**, were synthesized according to literature methods,[24c,30] as described in Scheme 1. The target compounds, **G1**, **G2**, and **G3**, were then prepared at moderate yields of 18–44% by the Ullmann C–N coupling reaction between 4,4′-diiodobiphenyl with an excess molar ratio of carbazole dendrons, **D1**, **D2**, and **D3**, respectively. They have good solubility in common organic solvents, such as dichloromethane, tetrahydrofuran and ethylacetate, such that they can be easily isolated and purified by column chromatography and recrystallization to reach high purity for spectroscopy characterization and OLED application. Their chemical structures were confirmed by ^{1}H and ^{13}C NMR spectroscopy, matrix-assisted laser desorption ionization time-of-flight (MALDI-TOF) mass spectrometry (Figures S1–3 in the Supporting Information), and elemental analysis.

2.2. Thermal Properties

The thermal properties of the dendrimers were investigated by means of thermogravimetric analysis (TGA) and differential scanning calorimetry (DSC) at a scanning rate of 10 °C min^{-1}; the data are listed in **Table 1**. As shown by the TGA curves in Figure S4 in the Supporting Information, **G2** and **G3** exhibit high thermal stability with decomposition temperatures (T_d) (corresponding to 5% weight loss) over 500 °C when heated in N_2, which are higher than that of **G1** (478 °C).

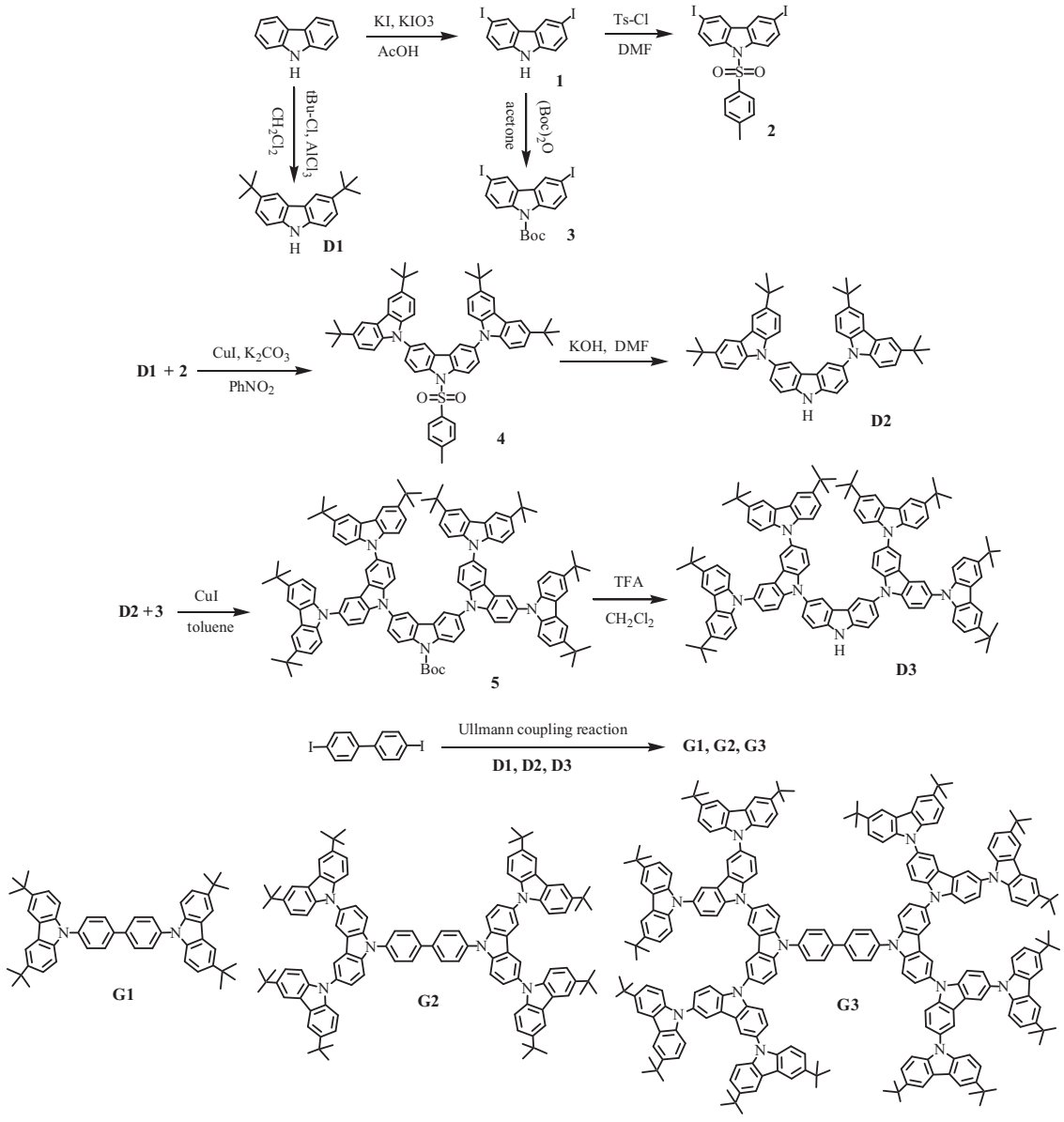

Scheme 1. Synthetic routes of the dendrimers: **G1**, **G2**, and **G3**.

This is an essential property for organic light-emitting materials especially when they are used at high temperature. The thermal stability is suggested to benefit at least partially from the presence of a large amount of carbazole groups, which are known to impart excellent thermal and chemical stability.[31] The morphological stability of these novel dendrimers was

Table 1. Summary of the physical parameters of the dendrimers.

Compound	λ_{max}^{abs} [nm]		λ_{max}^{em} [nm]		Φ [%][a)]	T_g [%]	T_d [°C]	HOMO [eV][c)]	E_g [eV][d)]	LUMO [eV]	E_T [eV][e)]
	CH_2Cl_2 [lg ε]	film	CH_2Cl_2	film							
G1	298(4.40),332(4.26)	299,337	396	403	80	175[b)]	478	–5.61	3.28	–2.33	2.62
G2	298(4.99),331(4.63)	298,336	401	408	17	300	502	–5.45	3.16	–2.29	2.60
G3	298(5.13),330(4.64)	299,335	400	407	14	376	517	–5.42	3.12	–2.30	2.61

[a)]Measured in CH_2Cl_2 solution with quinine sulfate as the standard ($\Phi = 0.55$ in 0.1 N H_2SO_4); [b)]The glass-transition temperature was obtained from Ref.[29]; [c)]Calculated with reference to ferrocene (4.8 eV); [d)]The optical band gap, calculated by the absorption edge technique; [e)]Measured in 2-MeTHF at 77 K.

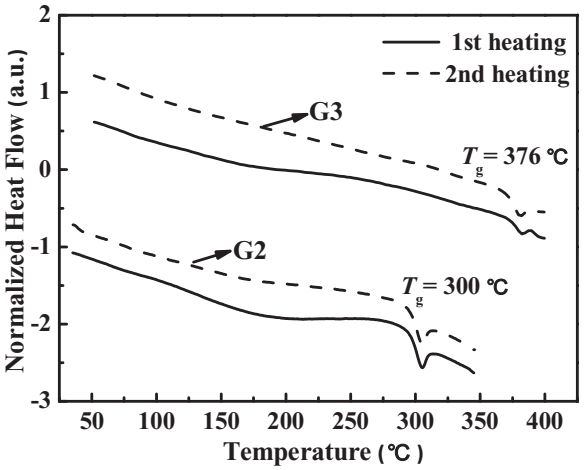

Figure 1. DSC traces of the **G2** and **G3** dendrimers (at a heating rate of 10 °C min^{-1}).

monitored by the DSC. As shown by the thermograms of **G2** in **Figure 1**, only one endothermic peak due to the glass transition was observed at 300 °C when a powder of **G2** was heated for the first run, implying that **G2** was amorphous even when it was obtained directly from organic solvents.[32] No obvious phase transition was detected when the sample was then cooled at a rate of either 50 or 10 °C min^{-1}. This endothermic glass transition was detected again when the sample was subsequently reheated. The thermograms of **G3** have similar features to those of **G2**, only one endothermic peak was observed at 376 °C, which is also assigned to the glass transition process. It was reported in literature that **G1** has a T_g of 175 °C.[29] Unfortunately, we did not detect such a glass transition process for **G1** under our own experimental conditions. It is, nevertheless, clear that the T_g of these dendrimers show a regular increasing trend with increasing dendron generation. The amorphous nature, even when obtained from organic solvents, and the high T_g over 300 °C for **G2** and **G3** indicate a high amorphous stability, which arises from their three-dimensional, molecular conformation due to the presence of the twisted biphenyl core and the bulky carbazole dendrons. It should be noted that such high T_g of 300 °C and 376 °C for **G2** and **G3** are among the highest ever reported for organic molecular materials.[33–35] By constructing vinyl-type polynorbornene with CBP side groups, Lee et al. developed a polymeric host for green PhOLEDs with a T_g of 361 °C, which is among the highest for conjugated and side-chain polymeric host materials.[33] Cheng et al. also reported three triptycene derivatives with high T_g values of 178–238 °C.[34] Recently Promarak and coworkers reported a carbazole dendronised triphenylamine molecule with the fourth generation carbazole dendrons possesses a T_g of as high as 401 °C, which was used as hole transporting layer in fluorescent OLEDs.[35] Evidently, the present **G3** shows the highest T_g value among all the host materials reported so far. Based on the excellent thermal and amorphous stability of these dendritic compounds, the possibility to prepare stable amorphous thin films from these compounds by solution casting is highly promising for applications in OLEDs.

2.3. Photophysical Properties

The photophysical properties of these dendrimers were investigated by means of electronic absorption and steady state photoluminescence (PL) measurements for both dilute solutions in dichloromethane and solid films on quartz plates. The pertinent data are summarized in Table 1. **Figure 2** shows the absorption and PL spectra of **G2** as an example. The absorption spectrum of **G2** in dilute solution exhibits two strong absorption bands in the ultraviolet region. The band peaked at 331 nm corresponds to the π–π^* electron transition of the entire conjugated backbone and the band at 298 nm could be assigned to the π–π^* local electron transition of the carbazole dendron at the terminal ends. A red shift of 5 nm was detected in the absorption spectrum of the **G2** thin film in comparison with its solution. Upon photoexcitation at the absorption maximum, the **G2** solution exhibits deep-blue fluorescence with an emission peak at 401 nm. Similar to the absorption, a red shift of 7 nm was detected in the PL spectra of the thin film. The absorption spectra of **G1** and **G3** (Figure S5, Supporting Information) have the similar features with those of **G2**. They exhibit deep-blue PL with emission peak at 396 nm in solution and 403 nm in the thin film for **G1**, and at 400 nm in solution and 407 nm in the thin film for **G3**. The bathochromic effect in both absorption

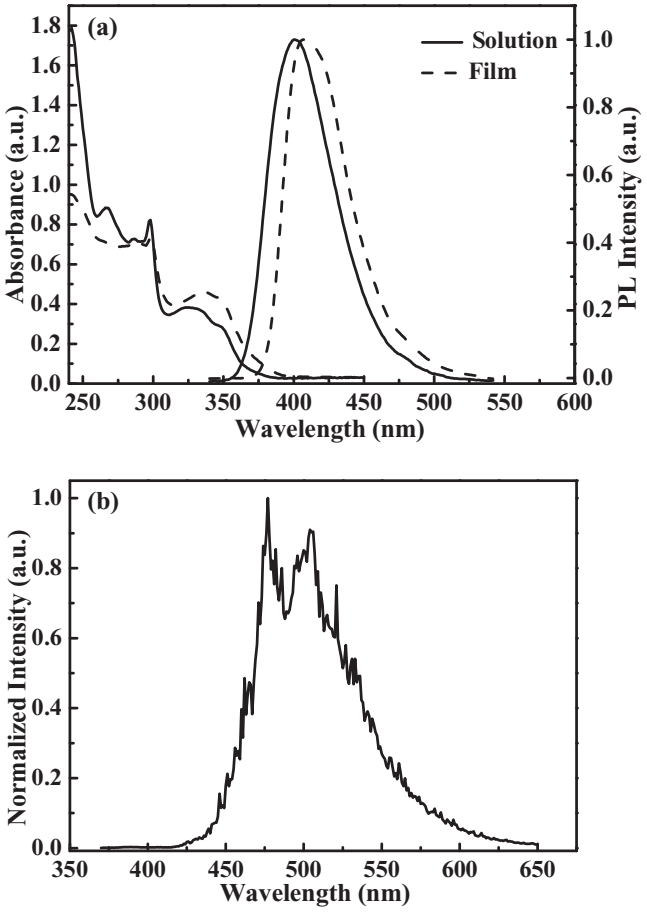

Figure 2. a) Absorption and fluorescence spectra of **G2** in dilute dichloromethane solution and in the solid state. b) Phosphorescence spectra of **G2** in 2-MeTHF at 77 K.

and PL spectra are frequently observed due to intermolecular interaction in solid state. However, the small red shift of only 5–7 nm in both absorption and PL spectra of these dendrimers reflects that the introduction of carbazole dendrons to the 4,4′-positions of the twisted biphenyl core further render the molecule in a nonplanar three-dimensional structure. Such a molecular conformation can effectively inhibit unwanted intermolecular interaction. The phosphorescence emission spectra of these dendrimers were measured in 2-MeTHF at 77 K; the phosphorescence spectrum of **G2** is illustrated in Figure 2b as an example. The peak wavelength of the highest energy 0-0 band was used to calculate the triplet excited state energy (E_T), giving the values of 2.62, 2.60, and 2.61 eV for **G1**, **G2**, and **G3**, respectively. It is obvious that these dendritic CBP derivatives have almost the same triplet energies as the parent CBP (measured as 2.67 eV under the same conditions),[36] indicating that such a molecular design strategy, by attaching higher generatioin carbazoles via their N-position to the 3,6-positions of inner carbazole moiety, does not significantly influence on the triplet energy of the whole dendrimer molecules. The triplet energies of these dendrimers are significantly higher than the values of the commonly used green-emitting phosphor $Ir(ppy)_3$ (2.41 eV, Hppy = 2-phenylpyridine)[33] and other longer-wavelength emitters. A higher value of E_T for the host material is a necessary provision for effective confinement of the triplet excitons on the guest by preventing back energy transfer from guest to the host molecules. In this case, these newly synthesized dendrimers with high triplet energy levels are expected to serve as appropriate hosts for green- and even longer-wavelength emitting dopants.

2.4. Electrochemical Properties

Cyclic voltammetry (CV) measurements were performed using a conventional three-electrode cell setup with 0.1 M tetra-*n*-butylammonium hexafluorophosphate (Bu_4NPF_6) as a supporting electrolyte in CH_2Cl_2, and ferrocene as the internal standard, to investigate the redox behavior of the dendrimers and to estimate their frontier molecular orbital levels. The cyclic voltamograms are shown in **Figure 3**. Upon the anodic sweep, **G1**, **G2**, and **G3** exhibit one, two, and three reversible oxidation processes, respectively. No reduction signal was detected for any of the dendrimers during the cathodic scan. As shown in Figure 3, the first oxidation waves of these dendrimers shift to less positive potentials, gradually with increasing dendrimer generation from **G1** to **G3**. This implies that the removal of the first electron from these dendritic molecules become easier with increasing dendron generation. This is consistent with the previous observation that the electron density increases on the outmost carbazole rings with increasing carbazole dendron generation.[30] The half-potential ($E^{1/2}$) of the first oxidation wave are in the range of 0.62–-0.81 V relative to ferrocene for these dendrimers. The HOMO energy levels were estimated from the values of $E^{1/2}$ to be –5.61, –5.45, and –5.42 eV for **G1**, **G2**, and **G3** respectively, according to the equation of HOMO (eV) = $-(E^{1/2}+ 4.8$ eV).[37] Apparently the HOMO levels of these carbazole-based dendrimers are higher than those of both CBP (–5.9 eV) and PVK (–5.8 eV) and quite close to the work function of the widely-used hole injecting material PEDOT:PSS (–5.2 eV),[17] implying that efficient hole injection into the emitting layer could be expected when these dendrimers are used as host materials in the emitting layer of OLEDs. The energy band gaps were determined by the absorption edge technique,[37] and the LUMO levels were calculated by subtracting the gap from the energy of the HOMO. Detailed electrochemical and electronic data of these molecules are listed in Table 1.

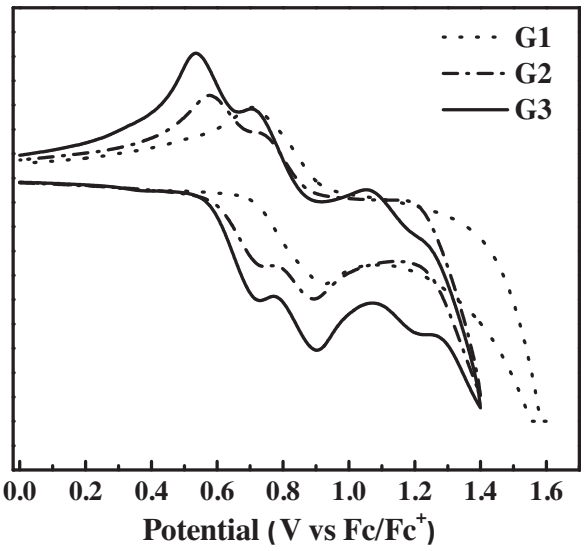

Figure 3. Cyclic voltammograms of **G1**, **G2** and **G3** measured in CH_2Cl_2 at a scan rate of 100 mV s^{-1}.

2.5. Electroluminescent Properties of OLEDs

In order to evaluate the performance of the dendrimers when used as hosts for phosphorescent emitters, three types of PHOLEDs (A, B, and C) were fabricated by doping the green or orange iridium complexes in the dendrimers as the emitting layer. Based on the good solubility and film-forming abilities of the dendrimers, the emitting layers of all the OLEDs in present study were made by spin coating the mixed solution of these dendrimers and a certain dopant. The green emitting $Ir(ppy)_3$ was first selected as the dopant to prepare devices of type A, which have the configuration of ITO/PEDOT:PSS (40 nm)/dendrimer: 6 wt% $Ir(ppy)_3$ (40 nm)/TPBI (40 nm)/LiF (1 nm)/Al (100 nm). In these devices, PEDOT:PSS was used as the hole-injecting layer, and TPBI is 1,3,5-tris[*N*-(phenyl)benzimidazole]-benzene and was deposited by vacuum thermal evaporation on top of the emitting layer to act as the electron-transporting and hole-blocking layer. Devices A1, A2, and A3 contained **G1**, **G2**, and **G3** as host materials in emitting layer, respectively. All these devices showed typical green emission at around 510 nm originating from the guest $Ir(ppy)_3$, as show by the EL spectra in Figure S6. The absence of any residual emission from the dendrimer hosts or TPBI layer even at high current densities suggests a complete energy transfer from these dendrimer hosts to the iridium dopant and the effective hole-blocking function of the TPBI layer in addition to its electron-transporting role.

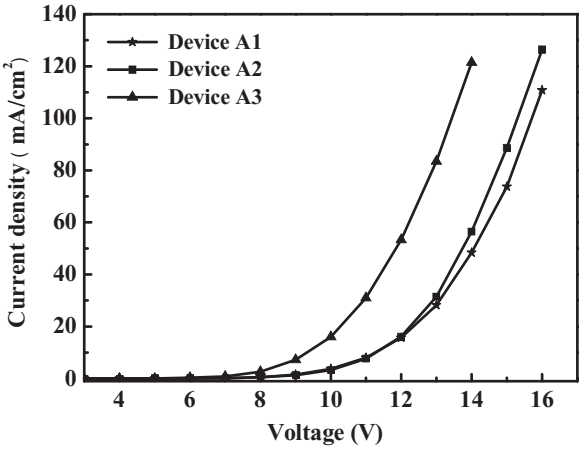

Figure 4. Current density-voltage (*J–V*) characteristics for devices A1, A2, and A3.

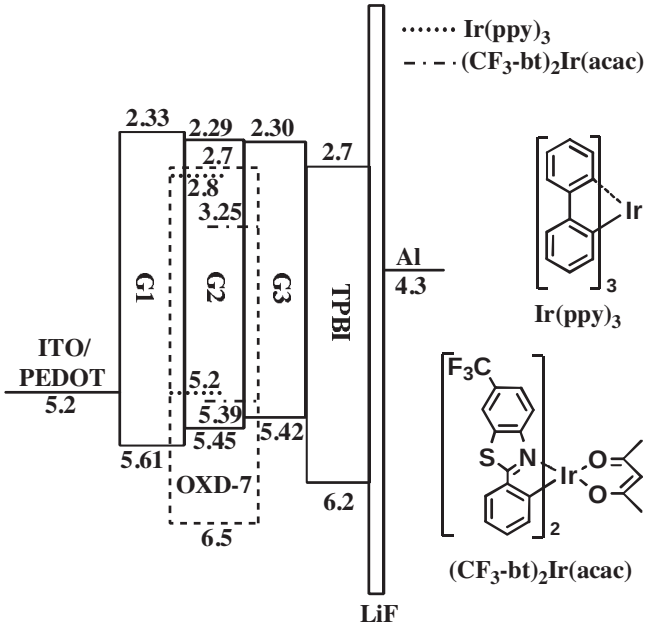

Figure 5. Left) Energy level diagram for the fabricated OLEDs. Right) Chemical structures of Ir(ppy)$_3$ and (CF$_3$-bt)$_2$Ir(acac).

Furthermore, there is no voltage dependence of the EL spectra over the whole applied voltage range. **Figure 4** displays the current density-voltage (*J–V*) characteristics of the three devices A1, A2, and A3. They turn on (to deliver a luminance of 1 cd m^{-2}) at 5.9, 5.1, and 4.8 V, respectively. The current density of these devices exhibited a regular variation in spite of the identical device configuration. With increasing dendrimer generation, the current density of the corresponding device at a given voltage increases regularly and the *J–V* curve shifts to lower voltages. This likely results from the facilitated hole injection in the devices containing the higher-generation dendrimer hosts. According to the energy level diagram in **Figure 5**, the relatively higher HOMO levels of **G2** (–5.45 eV) and **G3** (–5.42 eV) match the work function of the PEDOT (–5.2 e V) layer better than that of **G1**, resulting in a lower hole injection barrier at the PEDOT/dendrimer interface and thus a much lower driving voltage. The **G2** based device, A2, exhibited a maximum luminance of 11 991 cd m^{-2} at 16 V, and a maximum luminance efficiency η_L of 23.76 cd A^{-1}, corresponding to a peak power efficiency η_p of 8.22 lm W^{-1} and a forward-viewing external quantum efficiency η_{ext} of 7.01%. The **G3** based device, A3, achieved maximum efficiencies of 20.75 cd A^{-1}, 8.69 lm W^{-1} and 6.12% (Figure S7, Supporting Information). The efficiencies of the present three devices far exceed the best data available in the literature (15 cd A^{-1}) for a partially solution-processed phosphorescent device with a PVK:Ir(ppy)$_3$ emitting layer.[38] The detailed performances of these devices are summarized in **Table 2**.

Based on the good performance of device type A and the hole-transporting feature of these carbazole based dendrimer hosts, the electron-transporting component was introduced into

Table 2. EL data of the different OLED devices based on different dendrimers hosts and dopants.

Device[a)]	Host	Dopant	V_{on}[b)] [V]	L_{max}[c)] [cd m^{-2}, V]	η_L[c)] [cd A^{-1}, V]	η_p[c)] [lm W^{-1}, V]	η_{ext}[c)] [%]	CIE (x, y) at 8 V
A1	G1	Ir(ppy)$_3$	5.9	10930, 16	18.25, 10	6.36, 8	5.38	0.28, 0.62
A2	G2	Ir(ppy)$_3$	5.1	11991, 16	23.76, 10	8.22, 8	7.01	0.28, 0.63
A3	G3	Ir(ppy)$_3$	4.8	11300, 14	20.75, 8	8.69, 7	6.12	0.27, 0.62
B1	G1	Ir(ppy)$_3$	5.0	19220, 14	34.49, 9	13.15, 8	10.17	0.27, 0.62
B2	G2	Ir(ppy)$_3$	4.5	22020, 14	38.71, 8	15.69, 7	11.42	0.28, 0.63
B3	G3	Ir(ppy)$_3$	3.8	19820, 13	36.38, 7	18.59, 6	10.73	0.27, 0.62
B4	PVK	Ir(ppy)$_3$	5.0	12820, 15	27.70, 10	9.58, 9	8.17	0.28, 0.63
C1	G1	(CF3-bt)$_2$Ir(acac)	4.1	9745, 11	22.21, 5	13.94, 5	7.88	0.51, 0.47
C2	G2	(CF3-bt)$_2$Ir(acac)	3.9	12050, 11	32.22, 5	20.23, 5	11.44	0.51, 0.48
C3	G3	(CF3-bt)$_2$Ir(acac)	3.8	10810, 10	30.49, 5	19.15, 5	10.82	0.51, 0.48

[a)]Devices configurations, A: ITO/PEDOT:PSS (40 nm)/dendrimer: 6 wt% Ir(ppy)$_3$ (40 nm)/TPBI (40 nm)/LiF (1 nm)/Al (100 nm); B: ITO/PEDOT:PSS (40 nm)/dendrimer or PVK: 30 wt% OXD-7: 6 wt% Ir(ppy)$_3$ (40 nm)/TPBI (40 nm)/LiF (1 nm)/Al (100 nm); C: ITO/PEDOT:PSS (40 nm)/dendrimer: 30 wt% OXD-7: 8 wt% (CF3-bt)$_2$Ir(acac) (40 nm)/TPBI (40 nm)/LiF (1 nm)/Al (100 nm); [b)]Recorded at 1 cd/m^2; [c)]Maximum values of the devices. The values after the comma are the voltages at which the data are obtained.

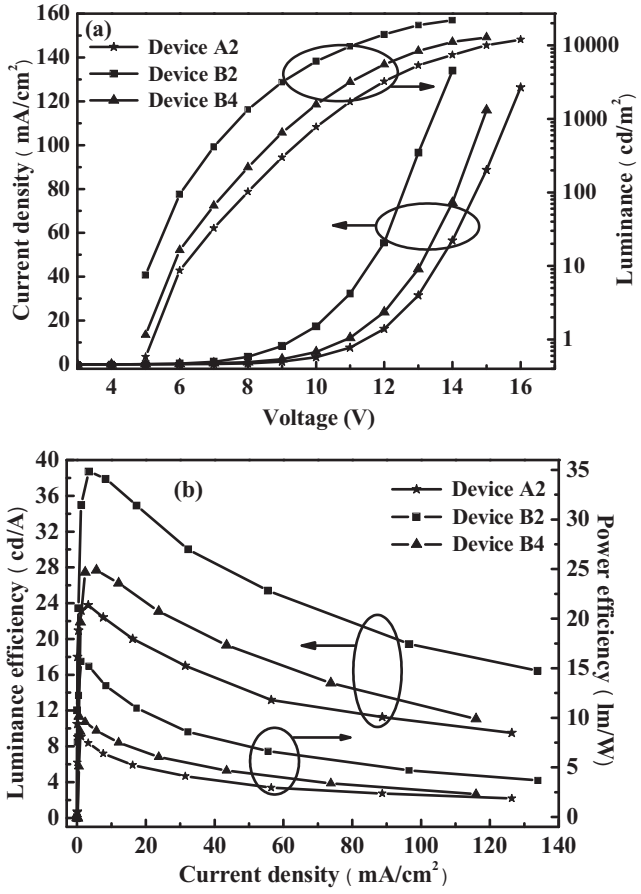

Figure 6. a) Voltage-current density-luminance (*V-J-L*) characteristics, and b) luminance efficiency and power efficiency as a function of current density for devices A2, B2, and B4.

the emitting layer of device type B to further facilitate charge transport balance and to improve device performance. Devices of type B have the structures ITO/PEDOT:PSS (40 nm)/dendrimer: 30 wt% OXD-7: 6 wt% Ir(ppy)$_3$ (40 nm)/TPBI (40 nm)/LiF (1 nm)/Al (100 nm). OXD-7 is 2,2′-(1,3-phenylene)bis[5-(4-tert-butylphenyl)-1,3,4-oxadiazole] and is incorporated into the host matrix to facilitate electron-injection due to its lower-lying LUMO level (–2.7 eV) than that of the dendrimers and to enhance the charge balance due on its electron-transporting capability. As shown in **Figure 6**, the **G2** based device, B2, exhibited a lower turn-on voltage and higher current density at a given voltage than device A2. At the same time, the maximum efficiencies of devices of type B are dramatically improved as well in comparison with type A devices. For example, the **G2** based device B2 achieved peak efficiencies of η_L = 38.71 cd A^{-1} and η_p = 15.69 lm W^{-1}, and the **G3** based device B3 exhibited similarly high values of 36.38 cd A^{-1} and 18.59 lm W^{-1}, much higher than those of the corresponding device A. The detailed EL data of these devices are summarized in Figure S8 and Table 2. For comparison, we also prepared a control device employing PVK as the host material with the same architecture of device B. The control device exhibited a turn-on voltage of 5 V and a maximum efficiency of 27.70 cd A^{-1}, which are comparable to the data for devices with similar structures reported in the literature.[39,40] For example, Nakamura et al. reported that their green PHOLEDs containing a PVK:OXD-7:Ir(ppy)$_3$ active layer achieved a maximum luminance efficiency of 24 and 31 cd A^{-1}, using Ca/Al and Cs/Al as the cathode material, respectively.[39] Figure 6 clearly illustrates the performance evolution by optimizing the device structure and utilizing the novel dendrimer host to replace the traditional PVK host. Like in many OLEDs, especially electrophosphorescent devices, efficiency roll-off was observed in these device with increasing current density, which can be typically attributed to a combination of triplet-triplet annihilation and field-induced quenching effects.[10b,22] Evidently, the **G2** and **G3** based devices show significantly improved performance, with lower turn-on voltages, higher brightness and emission efficiencies, as compared to those of PVK. Moreover, the comprehensive performance of present type B devices is superior to that of solution-processed green PHOLEDs containing dendrimer hosts,[24a] and also close to that of a solution-processed green device with dendritic iridium phosphor doped as small molecular host.[24d] It should be noted that the **G3** based devices A3 and B3 have lower turn-on voltages and higher power efficiencies than the corresponding devices A2 and B2 containing **G2**. This is likely because the **G3** host has a slightly higher HOMO level than **G2** and more efficient hole injection occurs at the PEDOT/**G3** interface. However, the luminance efficiencies and external quantum efficiencies for devices A3 and B3 were lower relative to those of devices A2 and B2. This is probably because the remarkably high hole current in **G3** based devices may lead to the imbalance of positive and negative charge carriers in the emitting layer, which may be unfavorable for a high charge-recombination efficiency. In balance, the device performance improvement with increasing dendrimer generation from **G2** to **G3** is not as great as from **G1** to **G2**. This indicates that **G2** may be the most suitable dendrimer generation for ideal device performance, considering the comparatively complicated synthesis for higher generation dendrimers.

In order to explore the versatility of the dendrimers as host materials for various color phorphors, the orange-emitting iridium complex, bis(2-phenyl-6-trifluoromethylbenzothiozolato)-iridium(acetylacetonate) [(CF3-bt)$_2$Ir(acac)], was also selected as a doped emitter to fabricate type C devices, with the configuration ITO/PEDOT:PSS (40 nm)/dendrimer: 30 wt% OXD-7: 8 wt% (CF3-bt)$_2$Ir(acac) (40 nm)/TPBI (40 nm)/LiF (1 nm)/Al (100 nm). All the devices C1–3 show orange emission peaked at 570 nm with CIE coordinates of (0.51, 0.48) exclusively from (CF3-bt)$_2$Ir(acac), as shown by the EL spectra in Figure S6 (Supporting information). The current density-voltage-luminance (*J–V–L*) characteristics and the efficiency curves of the orange electrophosphorescence for the type C devices are illustrated in **Figure 7** and the data are listed in Table 2. The current density and efficiencies of the type C devices follow a similar trend as observed for the type A and B devices with changing the dendrimer generation. The **G2** and **G3** based devices show maximum efficiency of 32.22 cd A^{-1}, 20.23 lm W^{-1} and 30.49 cd A^{-1}, 19.15 lm W^{-1}, respectively. Orange-emitting devices fabricated by spin-coating have rarely been reported in the literature.[41,42] For example, Schubert et al. presented solution-processed PhOLEDs using an orange-emitting crosslinkable iridium(III)

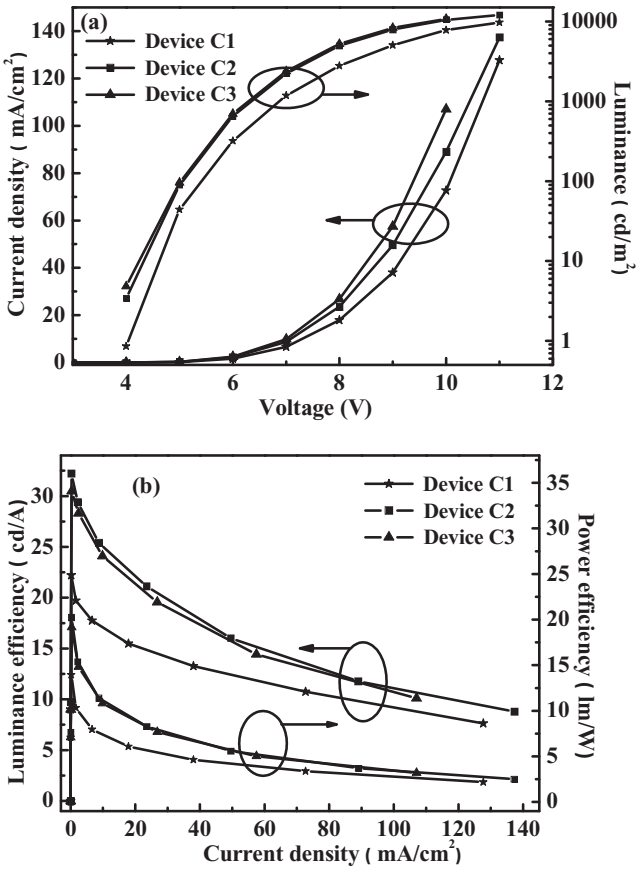

Figure 7. a) Voltage-current density-luminance (*V-J-L*) characteristics, and b) luminance efficiency and power efficiency as a function of current density for devices C1, C2, and C3.

complex as the dopant, reaching a maximum luminance efficiency of 18.4 cd A^{-1} (15.4 lm W^{-1}) with CIE coordinates of (0.55, 0.44).[41] Phosphorescent OLEDs with orange-emitting iridium complexes with efficiencies of 29.77 cd A^{-1} and 13.35 lm W^{-1} and CIE coordinates of (0.49, 0.50) were demonstrated by Wong et al.[42] The EL performances of the devices we present here are thus among the best ever reported for solution-processed orange PHOLEDs.

3. Conclusion

We have demonstrated the successful evolution of the traditional small molecular phosphorescent host CBP to its dendritic analogues, **G1**, **G2**, and **G3**, by incorporating oligo-carbazole dendrons to the biphenyl skeleton. These dendrimer hosts inherit similar HOMO and LUMO energy levels and identical triplet energies to the parent CBP, but are superior in the sense that they exhibit much higher thermal and amorphous stability with extremely high glass transition temperatures (300 °C and 376 °C for **G2** and **G3)**, and that they are solution-processible. In comparison with another widely-used phosphorescent host, PVK, which is also suitable for wet methods but with a much lower HOMO level, these dendritic hosts are improved because their higher HOMO levels guarantee efficient hole injection, and thus low driving voltages and high power efficiency in OLEDs. These novel dendrimer hosts are suitable for a wide color range of dopants from green to red. The solution-processed green and orange phosphorescent OLEDs containing these dendritic hosts and iridium complex dopants exhibited excellent performances, which greatly outweighed those containing the PVK host. Comparable device performances were obtained when increasing the dendron generation from **G2** to **G3**, despite the higher stabilities of **G3**. This indicates that the second generation should be the most preferred molecular dimension for these dendrimer hosts considering the more complicated synthesis for the higher generations. Given the ease of synthesis and some performance advantages over the traditional small molecular or polymeric phosphorescent hosts, these carbazole-based dendrimers will be perfect alternatives as triplet host materials for solution-processible OLEDs.

4. Experimental Section

General Information: Chemicals, reagents and solvents from commercial sources were of analytical or spectroscopy grade and used as received without further purification. ^{1}H and ^{13}C NMR spectra were recorded on a Varian INOVA spectrometer (400 or 100 MHz). Mass spectra were recorded on a GC-TOF MS (Micromass, UK) mass spectrometer for TOF-MS-EI and a MALDI micro MX (Waters, USA) for MALDI-TOF-MS. Elemental analyses were carried out on a Carlo-Eriba 1106 elemental analyzer. Thermogravimetry analyses (TGA) and differential scanning calorimetry (DSC) measurements were carried out using a Perkin–Elmer thermogravimeter (Model TGA7) and a Netzsch DSC 204 at a heating rate of 10 °C min^{-1} under a nitrogen atmosphere, respectively. The fluorescence and UV-vis absorption spectra measurements were performed on a Perkin-Elmer LS55 fluorescence spectrometer and a Perkin-Elmer Lambda 35 UV-visible spectrophotometer, respectively. The phosphorescence spectra of the dendrimers were measured in 2-MeTHF glasses at 77 K on a Horiba Jobin Yvon Fluoro Max-4 (TCSPC) instrument. Electrochemical measurements were made by using a conventional three-electrode configuration and an electrochemical workstation (BAS100B, USA) at a scan rate of 100 mV s^{-1}. A glassy carbon working electrode, a Pt-wire counter electrode, and a saturated calomel electrode (SCE) as the reference electrode were used. All measurements were made at room temperature on samples dissolved in dichloromethane, with 0.1 M tetra-n-butylammonium hexafluorophosphate (Bu_4NPF_6) as the electrolyte and ferrocene as the internal standard.

OLEDs Fabrication and Measurements: The precleaned ITO glass substrates (30 Ω sq^{-1}) were treated by UV-ozone for 20 min. PEDOT/PSS (Bayer AG) was spin-coated on pretreated ITO substrates from aqueous dispersion and baked at 120 °C for 1 h. Subsequently, a mixture of the Ir complexes and the host was spin-coated from chlorobenzene solution onto the PEDOT:PSS layer, the thickness of which was controlled as 40 nm by adjusting the solution concentration and the spin rate. The substrate was transferred into a vacuum chamber to deposit the TPBI layer with a base pressure less than 10^{-6} Torr (1 Torr = 133.32 Pa). Finally, the device fabrication was completed through thermal deposition of LiF (1 nm) and then capping with Al metal (100 nm) as cathode. The emitting area of each pixel is determined by overlapping of the two electrodes as 9 mm^2. The EL spectra, CIE coordinates, and current-voltage-luminance relationships of devices were measured with computer-controlled Spectrascan PR 705 photometer and a Keithley 236 source-measure-unit. The forward viewing external quantum efficiency (η_{ext}) was calculated by using the luminance efficiency, EL spectra and human photopic sensitivity. All measurements were carried out at room temperature.

Compounds Synthesis: The carbazole dendrons **D1**, **D2**, **D3** and their intermidiates **1**, **2**, **3**, **4**, **5** were synthesized according to the literature methods.[24c,30]

G1: A mixture of compound **D1** (1.51 g, 5.4 mmol), 4,4′-diiodobiphenyl (1.0 g, 2.5 mmol), Cu-bronze (80 mg, 1.25 mmol), and K_2CO_3 (2.4 g, 17.5 mmol) were added to a 3-necked flask, and then 18-crown-6 (165 mg, 0.625 mmol) and *o*-dichlorobenzene (70 mL) were added under a nitrogen atmosphere. After stirring for 36 h at 110 °C, the solvent was removed under reduced pressure. Ammonia solution (30 mL) was added and the mixture was stand for 2 h. Water was added and the mixture was extracted with dichloromethane. The combined organic phases were separated and washed with dilute HCl and brine, then dried over anhydrous $MgSO_4$. The solvent was removed to dryness and the residue was purified by column chromatography over silica gel with petroleum ether/dichloromethane (4:1) as the eluent to give **G1** as a white solid (700 mg, 40% yield).

^{1}H NMR (400 MHz, $CDCl_3$, δ): 8.15 (d, J = 8.4 Hz, 4H; ArH), 7.89 (d, J = 8.4 Hz, 4H; ArH), 7.69 (d, J = 8.8 Hz, 4H; ArH), 7.50-7.41 (m, 8H; ArH), 1.47 (s, 36H; CH_3); MALDI-TOF-MS (m/z): [M^+] calculated for $C_{52}H_{56}N_2$, 708.4443; Found, 708.0338. Analytically calculated for $C_{52}H_{56}N_2$: C, 88.09; H, 7.96; N, 3.95. Found: C, 88.17; H, 7.81; N, 3.86.

G2: A mixture of compound **D2** (1.02 g, 1.4 mmol), 4,4′-diiodobiphenyl (260 mg, 0.64 mmol), CuI (2.4 g, 0.128 mmol), K_3PO_4 (410 mg, 1.92 mmol) were added to a 2-necked flask, and then (±)-*trans*-1,2-cyclohexanediamine (1.7 µL, 0.014 mmol) and toluene (60 mL) were added under a nitrogen atmosphere. After stirring for 48 h at 110 °C, the reaction mixture was cooled to room temperature. The solvent was removed under reduced pressure, dichloromethane and water were added. The organic layer was separated and washed with dilute HCl and brine, then dried over anhydrous $MgSO_4$. The solvent was removed to dryness and the residue was purified by column chromatography over silica gel with petroleum ether/dichloromethane (3:1) as the eluent and then washed with petroleum ether to give **G2** as a white solid (450 mg, 44% yield).

^{1}H NMR (400 MHz, $CDCl_3$, δ): 8.28 (s, 4H; ArH), 8.18 (s, 8H; ArH), 8.07 (d, J = 8.4 Hz, 4H; ArH), 7.92 (d, J = 8.4 Hz, 4H; ArH), 7.77 (d, J = 8.8 Hz, 4H; ArH), 7.67-7.64 (m, 4H; ArH), 7.49-7.46 (m, 8H; ArH), 7.37 (d, J = 8.8 Hz, 8H; ArH), 1.47 (s, 72H; CH_3); ^{13}C NMR (400 MHz, $CDCl_3$, δ): 142.67, 140.39, 140.20, 139.83, 136.99, 131.13, 128.93, 127.68, 126.10, 124.18, 123.62, 123.22, 119.43, 116.29, 111.23, 109.14, 34.78, 32.09; MALDI-TOF-MS (m/z): [M^+] calculated for $C_{116}H_{116}N_6$, 1593.9295; Found, 1593.8462. Analytically calculated for $C_{116}H_{116}N_6$: C, 87.39; H, 7.33; N, 5.27. Found: C, 87.44; H, 7.21; N, 5.25.

G3: A mixture of compound **D3** (925 mg, 0.54 mmol), 4,4′-Diiodobiphenyl (100 mg, 0.25 mmol), CuI (9.5 mg, 0.05 mol), K_2CO_3 (240 mg, 1.75 mmol) in freshly distilled nitrobenzene (50 mL) was stirred at reflux under a nitrogen atmosphere for 72 h. After evaporation of the solvent under reduced pressure, water was added and the mixture was extracted with dichloromethane. The combined organic phases were washed with diluted HCl and brine, then dried over anhydrous $MgSO_4$. The solvent was removed to dryness and the residue was purified by column chromatography over silica gel with petroleum ether/dichloromethane (3:1) as the eluent and then recrystallized from methanol to give **G3** as a white solid (150 mg, 18% yield).

^{1}H NMR (400 MHz, $CDCl_3$, δ): 8.59 (s, 4H; ArH), 8.28 (s, 8H; ArH), 8.18 (s, 20H; ArH), 8.03 (d, J = 8.4 Hz, 4H; ArH), 7.94-7.88 (m, 8H; ArH), 7.68-7.61 (m, 16H; ArH), 7.47-7.43 (m, 16H; ArH), 7.36 (d, J = 8.4 Hz, 16H; ArH), 1.46 (s, 144H; CH_3); ^{13}C NMR (400 MHz, $CDCl_3$, δ): 142.59, 141.39, 141.13, 140.23, 130.85, 130.28, 129.18, 127.89, 126.07, 124.35, 123.85, 123,57, 123,15, 119.47, 116.24, 111.07, 109.11, 34.74, 32.05; MALDI-TOF-MS (m/z): [M^+] calculated for $C_{244}H_{236}N_{14}$, 3363.8965; Found, 3364.0522. Analytically calculated for $C_{244}H_{236}N_{14}$: C, 87.10; H, 7.07; N, 5.83. Found: C, 87.14; H, 6.98; N, 5.85.

Supporting Information

Supporting Information is available from the Wiley Online Library or from the author.

Acknowledgements

We thank the National Natural Science Foundation of China (21072026, 20923006), the Ministry of Education for the New Century Excellent Talents in University (Grant NCET-08-0074), the NKBRSF (2009CB220009), and the Fundamental Research Funds for the Central Universities (DUT12ZD211) for financial support of this work.

Received: May 16, 2012
Revised: August 9, 2012
Published online: September 10, 2012

[1] L. Flamigni, A. Barbieri, C. Sabatini, B. Ventura, F. Barigelletti, *Top. Curr. Chem.* **2007**, *281*, 143.
[2] B. Ma, P. I. Djurovich, M. E. Thompson, *Coord. Chem. Rev.* **2005**, *249*, 1501.
[3] M. A. Baldo, D. F. O'Brien, Y. You, A. Shoustikov, S. Sibley, M. E. Thompson, S. R. Forrest, *Nature* **1998**, *395*, 151.
[4] Y. Tao, Q. Wang, C. Yang, Q. Wang, Z. Zhang, T. Zou, J. Qin, D. Ma, *Angew. Chem. Int. Ed.* **2008**, *47*, 8104.
[5] S. Ye, Y. Liu, C. Di, H. Xi, W. Wu, Y. Wen, K. Lu, C. Du, Y. Liu, G. Yu, *Chem. Mater.* **2009**, *21*, 1333.
[6] L. Xiao, Z. Chen, B. Qu, J. Luo, S. Kong, Q. Gong, J. Kido, *Adv. Mater.* **2011**, *23*, 926.
[7] Y. Sun, N. C. Giebink, H. Kanno, B. Ma, M. E. Thompson, S. R. Forrest, *Nature* **2006**, *440*, 908.
[8] H. Wu, L. Ying, W. Yang, Y. Cao, *Chem. Soc. Rev.* **2009**, *38*, 3391.
[9] M. C. Gather, A. Köhnen, K. Meerholz, *Adv. Mater.* **2011**, *23*, 233.
[10] a) C. Jiang, W. Yang, J. Peng, S. Xiao, Y. Cao, *Adv. Mater.* **2004**, *16*, 537; b) H. Wu, G. Zhou, J. Zou, C.-L. Ho, W.-Y. Wong, W. Yang, J. Peng, Y. Cao, *Adv. Mater.* **2009**, *21*, 4181; c) H. Wu, J. Zou, D. An, F. Liu, W. Yang, J. Peng, A. Mikhailovsky, G. C. Bazan, Y. Cao, *Org. Electron.* **2009**, *10*, 1562.
[11] a) Y.-C. Chen, G.-S. Huang, C.-C. Hsiao, S.-A. Chen, *J. Am. Chem. Soc.* **2006**, *128*, 8549; b) X. Yang, D. C. Müller, D. Neher, K. Meerholz, *Adv. Mater.* **2006**, *18*, 948.
[12] J. H. Park, C. Yun, T.-W. Koh, Y. Do, S. Yoo, M. H. Lee, *J. Mater. Chem.* **2011**, *21*, 5422.
[13] J. Liu, Q. G. Zhou, Y. X. Cheng, Y. H. Geng, L. X. Wang, D. G. Ma, X. B. Jing, F. S. Wang, *Adv. Mater.* **2005**, *17*, 2974.
[14] C. H. Chien, S. F. Liao, C. H. Wu, C. F. Shu, S. Y. Chang, Y. Chi, P. T. Chou, C. H. Lai, *Adv. Funct. Mater.* **2008**, *18*, 1430.
[15] Z. Ma, J. Ding, B. Zhang, C. Mei, Y. Cheng, Z. Xie, L. Wang, X. Jing, F. Wang, *Adv. Funct. Mater.* **2010**, *20*, 138.
[16] A. van Dijken, J. J. A. M. Bastiaansen, N. M. M. Kiggen, B. M. W. Langeveld, C. Rothe, A. Monkman, I. Bach, P. össel, K. Brunner, *J. Am. Chem. Soc.* **2004**, *126*, 7718.
[17] N. Koch, A. Elschner, J. P. Rabe, R. L. Johnson, *Adv. Mater.* **2005**, *17*, 330.
[18] N. Koch, A. Kahn, J. Ghijsen, J.-J. Pireaux, J. Schwartz, R. L. Johnson, A. Elschner, *Appl. Phys. Lett.* **2003**, *82*, 70.
[19] L. Duan, L. Hou, T.-W. Lee, J. Qiao, D. Zhang, G. Dong, L. Wang, Y. Qiu, *J. Mater. Chem.* **2010**, *20*, 6392.
[20] M. Zhu, T. Ye, X. He, X. Cao, C. Zhong, D. Ma, J. Qin, C. Yang, *J. Mater. Chem.* **2011**, *21*, 9326.
[21] G. R. Newkome, C. N. Moorefield, F. Vögtle, *Dendritic Molecules: Concept, Synthesis and Perspectives*, Wiley-VCH, Weinheim, Germany **1996**.
[22] G. Zhou, W.-Y. Wong, B. Yao, Z. Xie, L. Wang, *Angew. Chem. Int. Ed.* **2007**, *46*, 1149.
[23] J. Ding, B. Zhang, J. Lü, Z. Xie, L. Wang, X. Jing, F. Wang, *Adv. Mater.* **2009**, *21*, 4983.
[24] a) J. Yang, T. Ye, Q. Zhang, D. Ma, *Macromol. Chem. Phys.* **2010**, *211*, 1969; b) J. Ding, J. Lü, Y. Cheng, Z. Xie, L. Wang, X. Jing, F. Wang, *Adv. Funct. Mater.* **2008**, *18*, 2754; c) H. Zhang, S. Wang,

Y. Li, B. Zhang, C. Du, X. Wan, Y. Chen, *Tetrahedron* **2009**, *65*, 4455; d) J. Ding, J. Cao, Y. Cheng, Z. Xie, L. Wang, D. Ma, X. Jing, F. Wang, *Adv. Funct. Mater.* **2006**, *16*, 575.
[25] Y.-S. Yao, J. Xiao, X.- S. Wang, Z.-B. Deng, B.-W. Zhang, *Adv. Funct. Mater.* **2006**, *16*, 718.
[26] M. A. Baldo, S. Lamansky, P. E. Burrows, M. E. Thompson, S. R. Forrest, *Appl. Phys. Lett.* **1999**, *75*, 4.
[27] K. Brunner, A. van Dijken, H. Börner, J. J. A. M. Bastiaansen, N. M. M. Kiggen, B. M. W. Langeveld, *J. Am. Chem. Soc.* **2004**, *126*, 6035.
[28] M. H. Tsai, Y. H. Hong, C. H. Chang, H. C. Su, C. C. Wu, A. Matoliukstyte, J. Simokaitiene, S. Grigalevicius, J. V. Grazulevicius, C. P. Hsu, *Adv. Mater.* **2007**, *19*, 862.
[29] M.-H. Ho, B. Balaganesan, T.-Y. Chu, T.-M. Chen, C. H. Chen, *Thin Solid Films* **2008**, *517*, 943.
[30] K. Albrecht, K. Yamamoto, *J. Am. Chem. Soc.* **2009**, *131*, 2244.
[31] J. Li, D. Liu, Y. Li, C.-S. Lee, H.-L. Kwong, S. Lee, *Chem. Mater.* **2005**, *17*, 1208.
[32] T. Zhang, D. Liu, Q. Wang, R. Wang, H. Ren, J. Li, *J. Mater. Chem.* **2011**, *21*, 12969.
[33] J. Park, C. Yun, T.-W. Koh, Y. Do, S. Yoo, M. Lee, *J. Mater. Chem.* **2011**, *21*, 5422.
[34] H.-H. Chou, H.-H. Shih, C.-H. Cheng, *J. Mater. Chem.* **2010**, *20*, 798.
[35] P. Moonsin, N. Prachumrak, R. Rattanawan, T. Keawin, S. Jungsuttiwong, T. Sudyoadsuk, V. Promarak, *Chem. Commun.* **2012**, *48*, 3382.
[36] C. Adachi, R. C. Kwong, P. Djurovich, V. Adamovich, M. A. Baldo, M. E. Thompson, S. R. Forrest, *Appl. Phys. Lett.* **2001**, *79*, 2082.
[37] D. Liu, H. C. Ren, J. Y. Li, Q. Tao, Z. X. Gao, *Chem. Phys. Lett.* **2009**, *482*, 72.
[38] H. M. Lee, S. J. Baek, S. C. Gong, C. D. Jeon, J. E. Chol, *Opt. Eng.* **2009**, *48*, 1040011.
[39] A. Nakamura, T. Tada, M. Mizukami, S. Yagyu, *Appl. Phys. Lett.* **2004**, *84*, 130.
[40] X. H. Yang, D. Neher, D. Hertel, T. K. Däubler, *Adv. Mater.* **2004**, *16*, 161.
[41] N. Rehmann, C. Ulbricht, A. Köhnen, P. Zacharias, M. C. Gather, D. Hertel, E. Holder, K. Meerholz, U. S. Schubert, *Adv. Mater.* **2008**, *20*, 129.
[42] C.-L. Ho, W.-Y. Wong, G.-J. Zhou, B. Yao, Z. Xie, L. Wang, *Adv. Funct. Mater.* **2007**, *17*, 2925.